J. Mol. Biol. (1976) **108**, 237–254

An Approach to the Organization of Eukaryotic Genomes at a Macromolecular Level

GABRIEL MACAYA, JEAN-PAUL THIERY† AND GIORGIO BERNARDI

Laboratoire de Génétique Moléculaire, Institut de Biologie Moléculaire Paris 75005, France

(Received 6 February 1976, and in revised form 21 June 1976)

DNAs from three mammals, two amphibians, two invertebrates and a unicellular eukaryote, enzymatically degraded to molecular weights in the 1×10^6 to 2×10^6 range, were analyzed in their sedimentation coefficients, and modal and mean buoyant density of their CsCl bands. These were further analyzed in terms of Gaussian curves; a more detailed analysis of these genomes was done using the combined Cs_2SO_4–Ag^+, CsCl approach of Thiery *et al.* (1976).

The major components of degraded mammalian DNAs were identical, in both buoyant densities and relative amounts, to those of the undegraded preparations, with only slight density shifts for some components. In contrast, the major components of degraded amphibian DNAs showed a very different pattern compared to the undegraded DNAs; changes in buoyant densities and amounts of some components, the disappearance of some components and the appearance of new components were observed. Finally, the degraded *Drosophila* and *Saccharomyces cerevisiae* DNAs were similar to the undegraded preparations in that no components could be resolved within the main bands.

Mouse DNA preparations ranging in molecular weight from $1{\cdot}8 \times 10^6$ to over 200×10^6 were examined. Only very slight changes in the relative amounts of some components seemed to take place in the $1{\cdot}8 \times 10^6$ to 66×10^6 molecular weight range; the buoyant densities of the components did not appear to vary in the size range, $1{\cdot}8 \times 10^6$ to over 200×10^6.

1. Introduction

Three years ago we reported (Filipski *et al.*, 1973) that the main band of calf DNA was formed by three discrete components having buoyant densities in CsCl equal to 1·697, 1·704 and 1·709 g/cm^3, and representing about 50%, 25% and 10% of the total DNA, respectively. More recent work in our laboratory (Thiery *et al.*, 1976) has shown that the discrete components first observed in calf DNA are in fact present in all the 11 mammalian genomes examined so far in our laboratory. Components similar in buoyant densities and relative amounts were also observed in avian DNAs, whereas different components appear to make up the main band of amphibian DNAs.

Since all observations mentioned so far concerned DNAs having molecular weights in the 5×10^6 to 20×10^6 range, two important questions raised by the existence of discrete components in the main band of DNAs from animals belonging to several

† Present address: The Rockefeller University, New York, N.Y., U.S.A.

phyla were the following: (1) up to which level of molecular weight could discrete components be seen or, in other words, at which DNA fragment size did the components begin to be interspersed with each other? (2) The discrete components as isolated at the 5×10^6 to 20×10^6 molecular weight level exhibited CsCl bands which were at least as symmetrical as bacterial DNAs of comparable molecular weights; yet they evidently had some degree of intramolecular compositional heterogeneity; at which molecular weight could this intramolecular heterogeneity be transformed into an intermolecular heterogeneity? Quite clearly both questions can be seen as a single one, namely what is the molecular size range where the discrete components exist? We have attempted in this work to give an answer to these questions by investigating, in terms of buoyant densities and relative amounts of components, eukaryotic DNAs either degraded to the 1×10^6 to 2×10^6 molecular weight range or prepared in such a way as to obtain fragment sizes in excess of 200×10^6.

2. Materials and Methods

DNA preparations, analytical density gradient centrifugation, analysis of CsCl band profiles, preparative density gradient centrifugation, and sedimentation velocity experiments have already been described (Thiery *et al.*, 1976).

DNA degradation with restriction enzymes was done as follows. DNA samples were dialyzed against 10 mM-NaCl and 6·6 mM each of $MgCl_2$, β-mercaptoethanol, Tris·HCl (pH 7·4). They were digested, at a concentration of 80 μg/ml, with *Hin*dII+III (Smith & Nathans, 1973), a mixture of restriction enzymes II and III from *Haemophilus influenzae* strain d; this was prepared according to Kopecka (1975). Degradation was carried out, at an enzyme concentration of 0·01 units/50 μg DNA (units as defined by Smith & Wilcox, 1970), in a capillary viscometer, at 36°C, until a viscosity plateau was reached. Alternatively, completion of digestion was controlled by 2 sedimentation velocity experiments done at the end of digestion (as estimated from viscosity) and after further incubation with an additional amount of enzyme, respectively. Degraded DNA samples (5 to 10 A_{260} units) were filtered through a 1·2 cm × 40 cm G25 column, equilibrated with 5 mM-borate buffer (pH 9·2) to transfer DNA into the solvent used in analytical and preparative density gradient centrifugation.

In addition to 3 mammalian, 2 amphibian, 1 invertebrate and an *Escherichia coli* DNA preparations degraded by restriction enzymes, 2 DNA samples from *Cancer pagurus* and *Saccharomyces cerevisiae*, respectively, were investigated here. These preparations had molecular weights of $1\cdot6\times10^6$ because of a random endogenous degradation. The nuclear DNA from *S. cerevisiae* was obtained from wild-type strain A as a by-product of mitochondrial DNA preparation (Bernardi *et al.*, 1972); the satellite DNA having a buoyant density of 1·705 g/cm^3 was removed by chromatography on hydroxyapatite.

Very high molecular weight ($>200\times10^6$) DNA preparations were obtained and analyzed by sedimentation in CsCl density gradients as follows. Thymus glands from 5 to 8-week old mice were cut into small fragments; these were suspended in 0·075 M-NaCl, 0·024 M-EDTA (pH 8·0) (Zubay & Doty, 1959); connective tissue debris sedimented very rapidly and the cell suspension was decanted. Cells were counted, after an appropriate dilution, in a Thoma chamber or in a Coulter counter; a volume of cell suspension (10 to 50 μl) containing 5×10^4 to 5×10^5 cells was pipetted on the bottom of the centerpiece of an analytical ultracentrifuge double-sector cell; the cell was then assembled, and loaded with 13 μl NL-30 Sarkosyl (Ciba–Geigy, Paris, France) and a CsCl solution in order to have a total volume of 0·4 ml and a density of 1·700 g/cm^3. The cell was gently rocked, and centrifuged at 40,000 revs/min for 48 h at 25°C. Experiments in which 10 μg of Proteinase K (Merck, Darmstadt, Germany) was added together with Sarkosyl, and the cell was incubated for 3 h at 37°C, gave identical results. This procedure appears to be very useful for an accurate determination of *c*-value (genome size or DNA content per haploid cell).

3. Results and Discussion

(a) *CsCl band analysis*

Table 1 shows the sedimentation coefficients, modal and mean buoyant densities in CsCl, ρ_0, $\langle\rho\rangle$, and the $\langle\rho\rangle - \rho_0$ values, as determined on seven DNA preparations both before and after restriction enzyme degradation. After enzymatic digestion, the sedimentation coefficients were in the 10·2 to 13 S range; this corresponds to molecular weights of 1×10^6 to 2×10^6, using the Eigner & Doty (1965) relationship. The $\langle\rho\rangle$

TABLE 1

Properties of DNAs before and after degradation by the restriction endonucleases Hind*II + III*†

DNA source Species	Tissue	$s_{20,w}$	ρ_0‡ (g/cm³)	$\langle\rho\rangle$‡ (g/cm³)	$\langle\rho\rangle - \rho_0$ (mg/cm³)
Homo sapiens (man)	Placenta	22·3	1·6990	1·7011	2·1
		13·0	1·6995	1·7011	1·6
Bos taurus (calf)	Liver	25·2	1·7000	1·7039	3·9
		13·7	1·7005	1·7037	3·2
	Thymus	26·0	1·6997	1·7033	3·6
		12·5	1·7001	1·7032	3·1
Mus musculus (mouse)	Liver	24·5	1·7007	1·7008	0·1
		12·5	1·7008	1·7008	0
Xenopus laevis	Erythrocytes	35	1·6991	1·6997	0·6
		10·7			
Pleurodeles waltlii	Testes	27·1	1·7041	1·7047	0·6
		12·9	1·7042	1·7048	0·6
Cancer pagurus§	Testes	11	1·7023	1·6997	−4·6
				1·7029	0·6¶
Drosophila melanogaster	Embryos	27·4	1·7025	1·7014	−1·1
		10·2	1·7029	1·7016	−1·3
Saccharomyces cerevisiae§	Nuclear	11	1·6995	1·7001	0·6
Escherichia coli		34·6	1·7105	1·7101	−0·4
		22·6‖	1·7106	1·7101	−0·5
		11·3	1·7104	1·7101	−0·3

† For each DNA, the upper and lower row of values concern undegraded and degraded samples, respectively. Values for undegraded DNAs are taken from the accompanying paper.

‡ The error on the ρ_0 values is $\pm0{\cdot}0005$ g/cm³; that on the $\langle\rho\rangle$ value is $\pm0{\cdot}0002$ g/cm³.

§ Values for *C. pagurus* and *S. cerevisiae* are for low molecular weight preparations, not degraded by *Hin*dII + III.

¶ The second line in *C. pagurus* corresponds to $\langle\rho\rangle$ and $\langle\rho\rangle - \rho_0$ values for main band DNA, not taking into account the contribution of the light satellite.

‖ This DNA sample was obtained by syringe shearing of the 34·6 S sample.

values are identical for the two series of samples, as expected. The ρ_0 values of undegraded and degraded DNAs are the same within experimental error; a trend towards slightly higher value is, however, apparent; this is due to the broadening of the components of the band.

(b) *Fractionation in preparative Cs_2SO_4–Ag^+ density gradients, and CsCl analysis of the fractions*

Figures 1 to 5 show the result obtained for human, mouse, calf, *Xenopus*, *Pleurodeles*, *Cancer*, *Drosophila*, *Saccharomyces* and *E. coli* DNA. The analysis of the CsCl

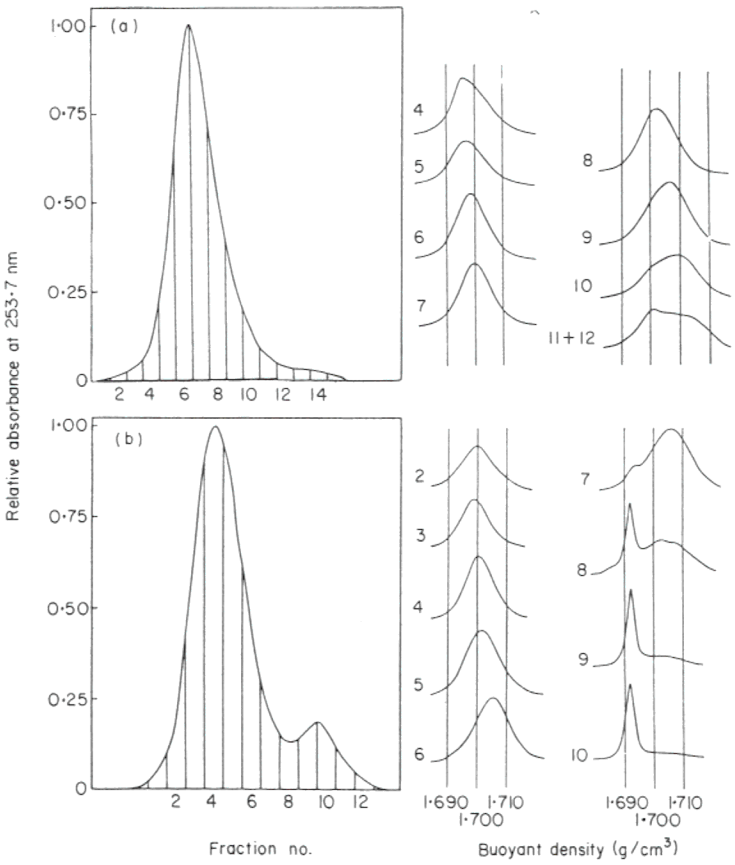

FIG. 1. Analysis of man and mouse DNA components in Cs_2SO_4–Ag^+ density gradient after degradation by *Hin*dII + III.

(a) Human placenta DNA ($A_{260nm} = 0{\cdot}49$) in borate buffer (pH 9·2) containing $AgNO_3$ ($r = 0{\cdot}32$) and Cs_2SO_4 ($\rho = 1{\cdot}50$ g/cm^3) was centrifuged in a type 65 rotor at 35,000 revs/min for 64 h.

(b) Degraded mouse liver DNA ($A_{260nm} = 0{\cdot}5$) in borate buffer (pH 9·2) containing $AgNO_3$ ($r = 0{\cdot}27$) and Cs_2SO_4 ($\rho = 1{\cdot}50$ g/cm^3) was centrifuged as described above.

band profiles of Cs_2SO_4–Ag^+ fractions in terms of Gaussian curves has been done as described in Appendix, section (a). The results obtained are summarized in Table 2.

(i) *DNAs from vertebrates*

A comparison of the data of Table 2 with those of Table 2 of the accompanying paper showed that the major components of the degraded mammalian DNAs were identical, in both buoyant densities and relative amounts, to those of the undegraded samples; slight but significant density shifts were found, however, for the 1·697, 1·704, and 1·709 g/cm^3 components of human DNA and the 1·709 g/cm^3 component of mouse DNA. In contrast with mammalian DNAs, the major components of degraded amphibian DNAs showed a very different pattern compared to the undegraded DNAs: some components showed slight changes in both buoyant densities

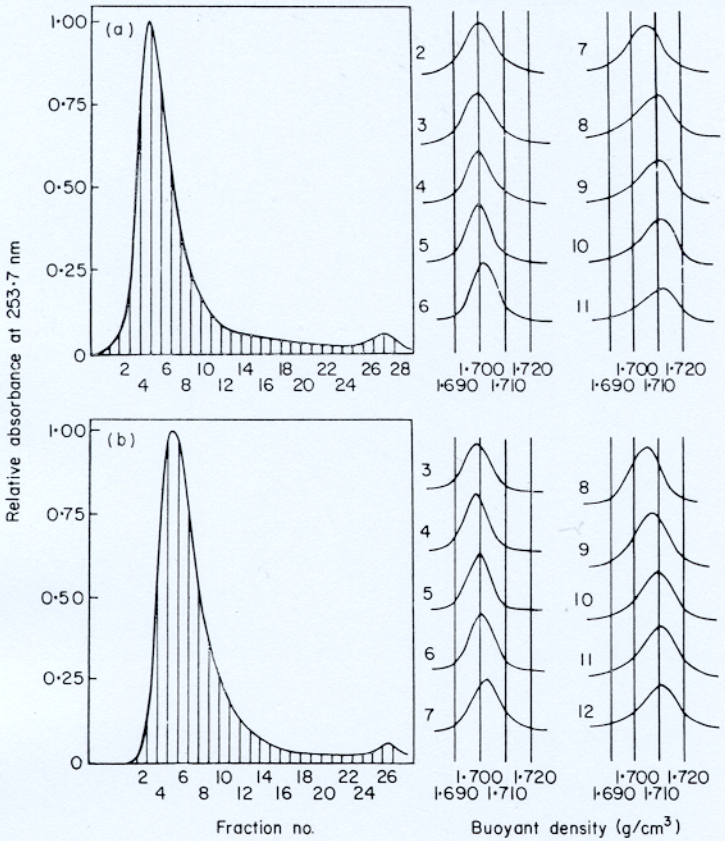

FIG. 2. Analysis of calf liver and calf thymus DNA components in Cs_2SO_4–Ag^+ density gradient after degradation by *Hin*dII + III.

(a) Calf liver DNA (A_{260nm} = 0·34) in borate buffer (pH 9·2) containing $AgNO_3$ (r = 0·35) and Cs_2SO_4 (ρ = 1·50 g/cm³) was centrifuged in a type 30 rotor at 25,000 revs/min for 110 h.

(b) Calf thymus DNA (A_{260nm} = 0·36) in borate buffer (pH 9·2) containing $AgNO_3$ (r = 0·35) and Cs_2SO_4 (ρ = 1·50 g/cm³) was centrifuged as described above.

and amounts and, more strikingly, restriction enzyme degradation caused the disappearance of some components (1·706 g/cm³ of *X. laevis*; 1·705 and 1·706 g/cm³ of *P. waltlii*) and the appearance of new components (1·7023 g/cm³ of *X. laevis*; 1·702 and 1·709 g/cm³ of *P. waltlii*). In addition the buoyant density range of the components present in degraded samples broadened considerably compared to the undegraded ones. Histograms showing the changes in buoyant densities and relative amounts of major components of vertebrate DNAs are presented in Figure 6.

As far as satellite DNAs† are concerned, some of them apparently were not degraded or only very partially degraded (human satellites 1·695 and 1·700 g/cm³, Fig. 1, fractions 4 and 11 + 12; calf satellites 1·705 and 1·723 g/cm³; mouse satellite 1·6915 g/cm³) as shown by the appearance of the corresponding bands; other ones were degraded and were difficult to recognize as satellites in the digested DNAs (human satellite 1·687 g/cm³, Fig. 1, absent in fraction 11 + 12; calf satellites

† For the sake of convenience, we will distinguish here the minor and satellite components, the latter corresponding to simple-sequence or highly repetitive DNAs.

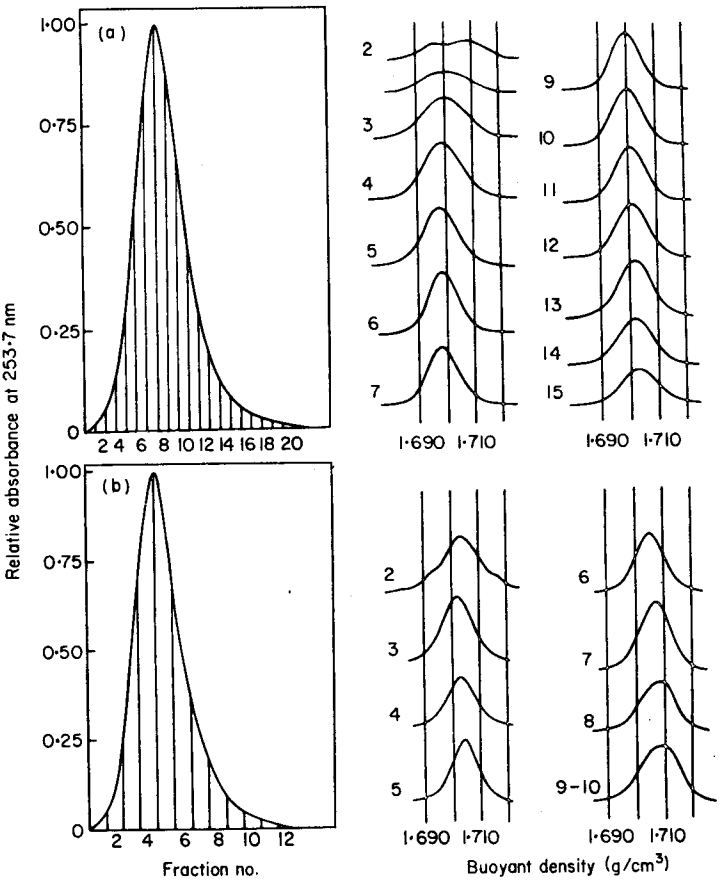

FIG. 3. Analysis of *Xenopus* and *Pleurodeles* DNA components in Cs_2SO_4–Ag^+ density gradient after degradation by *Hin*dII + III.

(a) *Xenopus* erythrocytes DNA (A_{260nm} = 0·36) in borate buffer (pH 9·2) containing $AgNO_3$ (r = 0·35) and Cs_2SO_4 (ρ = 1·50 g/cm³) was centrifuged in a type 30 rotor at 25,000 revs/min for 110 h.

(b) *Pleurodeles* testes DNA (A_{260nm} = 0·47) in borate buffer (pH 9·2) containing $AgNO_3$ (r = 0·35) and Cs_2SO_4 (ρ = 1·50 g/cm³) was centrifuged in a type 65 rotor at 35,000 revs/min for 64 h.

1·710 and 1·715 g/cm³). Concerning the minor components, some do not seem to change in buoyant density and relative amount (human 1·716 g/cm³; probably, calf 1·713 g/cm³; mouse 1·700 g/cm³); other ones cannot be recognized anymore (human 1·7135 g/cm³; calf 1·715 g/cm³; mouse 1·704 g/cm³); finally some new minor components appear after degradation (human 1·695 g/cm³; calf 1·700 g/cm³; mouse 1·691 g/cm³).

In the case of amphibian DNAs, the 1·712 g/cm³ satellite of *Xenopus* is still clearly evident (Fig. 3, fraction 2) as are the 1·686 g/cm³ and 1·716 g/cm³ satellites of *Pleurodeles* (Fig. 3, fraction 2); a new satellite, not detected in the undegraded DNA seems to appear in the degraded *Xenopus* DNA, at a density of 1·697 g/cm³ (Fig. 3, fractions 2 and 3). For the *Pleurodeles* DNA a number of new minor components appeared.

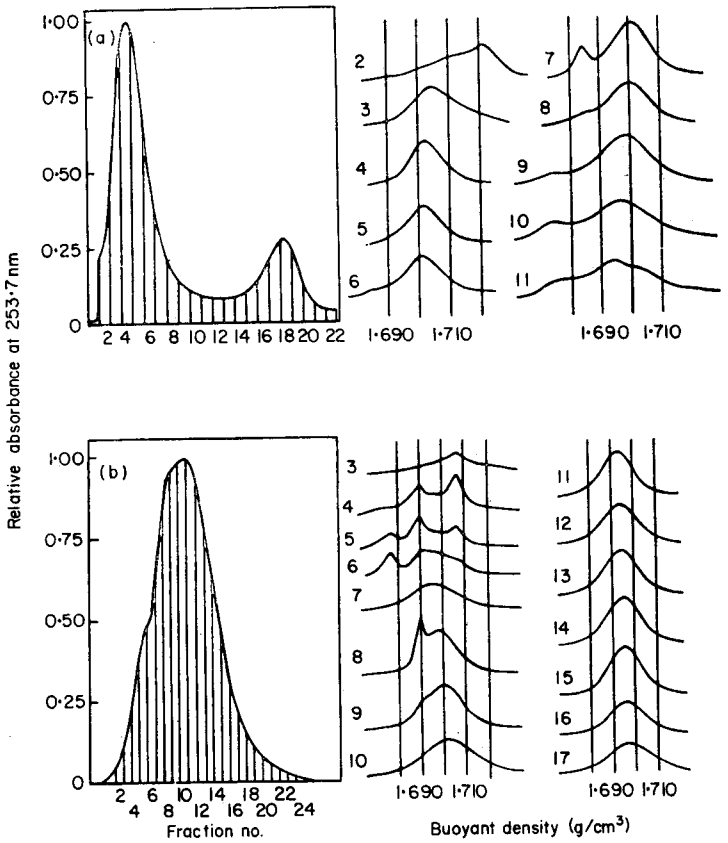

FIG. 4. Analysis of *C. pagurus* and *D. melanogaster* DNA components in Cs_2SO_4–Ag^+ density gradient.

(a) *Cancer* testes DNA (A_{260nm} = 0·95) in borate buffer (pH 7·9) containing $AgNO_3$ (r = 0·3) and Cs_2SO_4 (ρ = 1·47 g/cm³) was centrifuged in a type 30 rotor at 25,000 revs/min for 110 h.

(b) *Drosophila* embryo DNA degraded by *Hin*dII + III (A_{260nm} = 0·20) in borate buffer (pH 9·2) containing $AgNO_3$ (r = 0·35) and Cs_2SO_4 (ρ = 1·50 g/cm³) was centrifuged as described above.

(ii) *DNAs from invertebrates and yeast*

The major components of *Cancer* DNA were characterized by densities of 1·695, 1·701 and 1·708 g/cm³, and represented 10%, 52% and 10% of the genome, respectively. Three components of *Cancer* DNA correspond to previously described satellites (1·680 g/cm³, Fig. 4, fractions 16 to 20; and 1·721 g/cm³, Fig. 4, fraction 2) and to mitochondrial DNA (1·685 g/cm³, Fig. 4, fraction 7), respectively (Skinner, 1967; Skinner & Kerr, 1971).

As far as *Drosophila* DNA is concerned, no components could be resolved within the main band; the buoyant density in CsCl of main band fractions increased regularly for subsequent fractions and the band width corresponded to that expected on the basis of the molecular weight. The four *Drosophila* satellites were all seen in the degraded sample. Their buoyant densities (1·675, 1·689, 1·690 and 1·706 g/cm³, Fig. 4, fractions 3 to 9) and their relative amounts were in good agreement with those reported by Peacock *et al.* (1973) for high molecular weight DNA.

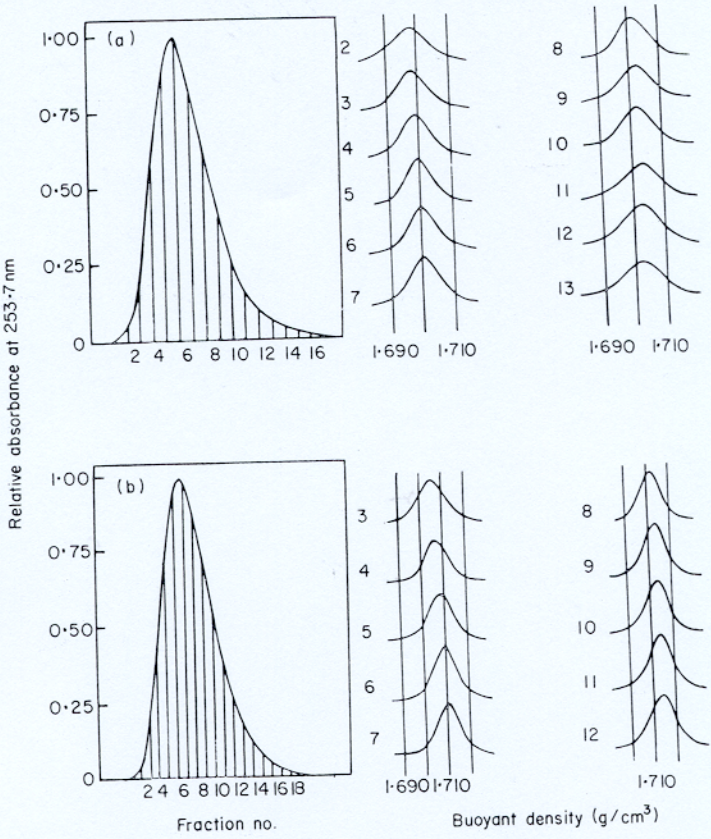

FIG. 5. Analysis of *S. cerevisiae* and *E. coli* DNA components in Cs_2SO_4–Ag^+ density gradient.

(a) Nuclear *S. cerevisiae* wild-type A DNA ($A_{260nm} = 0{\cdot}23$) in borate buffer (pH 9·2) containing $AgNO_3$ ($r = 0{\cdot}35$) and Cs_2SO_4 ($\rho = 1{\cdot}50$ g/cm³) was centrifuged in a type 30 rotor at 25,000 revs/min for 100 h.

(b) *E. coli* DNA degraded by *Hin*dII + III ($A_{260nm} = 0{\cdot}26$) in borate buffer (pH 9·2) containing $AgNO_3$ ($r = 0{\cdot}35$) and Cs_2SO_4 ($\rho = 1{\cdot}50$ g/cm³) was centrifuged as described above.

Yeast DNA could not be resolved into separate components; Cs_2SO_4–Ag^+ fractions were characterized by practically Gaussian profiles with regularly increasing densities ranging from 1·699 to 1·701 g/cm³. In contrast with *Drosophila* and *E. coli* DNA, the range of buoyant densities in CsCl of Cs_2SO_4–Ag^+ fractions was extremely narrow for yeast DNA.

(c) *Analysis of CsCl band patterns*

Since previous work (Thiery *et al.*, 1976) had shown that a simple Gaussian analysis of the CsCl band profiles of eukaryotic DNAs gave results in good agreement with the more elaborate procedure just described, such an analysis was also done on some of the degraded DNA preparations studied here. The results (Table 3) showed a satisfactory agreement with the analysis of Table 2 and encouraged us to perform the same type of analysis on DNA preparations differing in molecular weight (see the following section).

TABLE 2

Component patterns of degraded eukaryotic DNAs (combined Cs_2SO_4–Ag^+ and CsCl analysis)

Species	DNA source: Tissue	Major components (ρ)	Major components (%)	Minor components (ρ)	Minor components (%)	Satellites (ρ)	Satellites (%)
Homo sapiens	Placenta	1·6965	16 } 62	1·695	2·5		
		1·699	46 }	1·716	1	1·695	1·2
		1·7045	19			1·700	0·5
		1·710	9				
Bos taurus	Thymus	1·697	18 } 55	1·700	2·5	1·705	4
		1·700	37 }	1·713	3·5	1·710	3
		1·704	15			1·715	7
		1·709	13			1·723	0·5
	Liver	1·699	52	1·700	2·5	1·705	4
		1·704	15	1·713	4	1·710	3
		1·709	12			1·715	7
						1·723	0·5
Mus musculus	Liver	1·699	37 } 58	1·691	3·2	1·6915	7
		1·7015	21 }	1·693	0·5		
		1·7045	18	1·700	2		
		1·7095	8				
Xenopus laevis	Erythrocytes	1·6985	57	1·705	2	1·697	0·5
		1·700	24			1·712	0·3
		1·701	10				
		1·7023	6				
Pleurodeles waltlii	Testes	1·702	27·5	1·694	0·4	1·686	0·4
		1·7045	53·5	1·701	3	1·716	0·2
		1·709	11	1·706	3		
				1·7135	0·7		
Cancer pagurus	Testes	1·695	10			1·680	22
		1·701	52			1·685	0·5
		1·708	10			1·721	3
Drosophila melanogaster	Embryos	1·697–1·707†	82			1·675	3·7
						1·689	2·5
						1·690	5·2
						1·706	6·6
Saccharomyces cerevisiae	Nuclear	1·698–1·701†	100				
Escherichia coli		1·702–1·714†	100				

† The range of ρ values given here refers to the lowest and highest buoyant density in CsCl of Cs_2SO_4–Ag^+ fractions. The extreme values concern material representing less than 1% of total DNA.

(d) *Analysis of CsCl band patterns of mouse DNA preparations having different molecular weights*

The sedimentation coefficients, molecular weights, ρ_0, $\langle\rho\rangle$, and $\langle\rho\rangle - \rho_0$ values obtained for four mouse DNA preparations having molecular weights comprised between $1{\cdot}8\times10^6$ and over 2×10^8 are given in Table 4, which also presents $\langle\rho\rangle$, and $\langle\rho\rangle - \rho_0$ values, as calculated for main band DNA, not taking into account the contribution of the light satellite.

The practically identical component patterns (Table 5 and Fig. 7) obtained by CsCl band profile analysis of mouse DNA at two different molecular weight levels

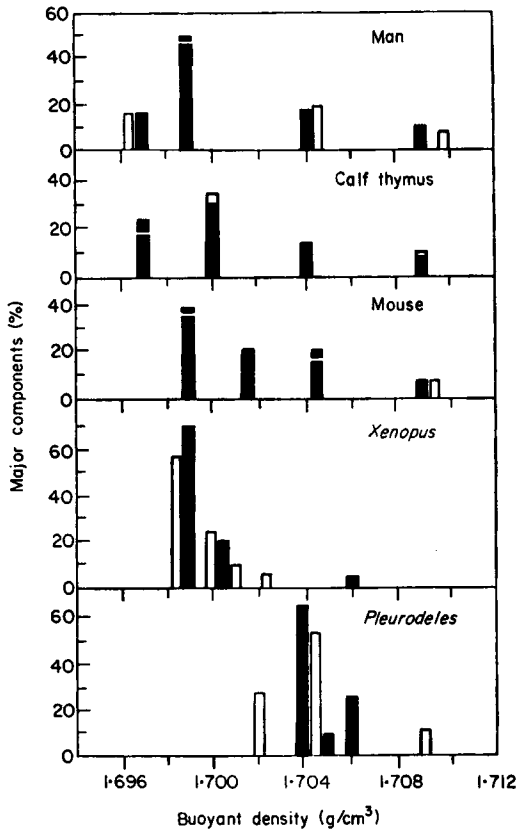

FIG. 6. Histogram of major components shown by 3 mammalian and 2 amphibian DNAs before and after degradation by *Hin*dII + III. Solid and open bars represent the relative amount of major component of undegraded and degraded DNA, respectively. Breaks on solid bars show the levels of degraded components when no shift in buoyant density took place.

(8×10^6 and 66×10^6) indicates that no changes in compositional heterogeneity take place in this molecular weight range.

As far as the molecular weight of the largest size sample is concerned, it should be stressed that the value of 200×10^6 is an underestimate. In fact, this molecular weight has been calculated from the total variance of the peak, assuming (see above) that the compositional heterogeneity of this sample was the same as those of the 11×10^6 and 66×10^6 DNAs, namely 4% G + C (this value was calculated using eqn (2) of Appendix, section (b)); since the concentration dependence of variance (see Appendix, section (b)) was not taken into account, the calculated molecular weight could only be underestimated.

Figure 8 shows the band profiles of the four mouse DNA preparations. As far as the main band is concerned, increasing the molecular weight from that of usual DNA preparations (in this case, 11×10^6) to 66×10^6 and to over 200×10^6 leads to the progressive appearance of accidents in the profile. In the highest size sample, where this phenomenon is particularly evident, accidents correspond to the buoyant densities of the components resolved by Cs_2SO_4–Ag^+ centrifugation, namely 1·699, 1·7015, 1·7045, and 1·709 g/cm³. On the other hand, degradation of DNA to $1{\cdot}8\times10^6$

TABLE 3

Component patterns of degraded eukaryotic DNAs (CsCl analysis)

DNA source Species	Tissue	Major components (ρ)	(%)	Minor components and satellites (ρ)	(%)
Homo sapiens	Placenta	1·6965	17 } 55	1·690	5
		1·699	38 }	1·7135	2
		1·704	19	1·718	2
		1·709	12		
Bos taurus	Thymus	1·697	16 } 56	1·705	4
		1·700	40 }	1·710	3
		1·704	15	1·7155	7
		1·709	11	1·712	1
	Liver	1·699	50	1·705	4
		1·704	20	1·710	3
		1·709	10	1·715	7
				1·722	1
Mus musculus	Liver	1·699	35 } 53	1·6912	8
		1·7015	18 }	1·6915	8
		1·7045	18	1·714	2
		1·7095	9		
Cancer pagurus		1·693	8	1·680	22
		1·7015	52	1·695	2
		1·708	10	1·721	3

TABLE 4

CsCl band profile analysis of mouse DNAs having different molecular weights

DNA source	$s_{20,w}$	M_w† ($\times 10^{-6}$)	ρ_0‡ (g/cm^3)	$\langle\rho\rangle$‡ (g/cm^3)	$\langle\rho\rangle - \rho_0$ (mg/cm^3)
Thymus	—	>200	—	1·7008	—
Thymus	50	66·2	1·7000	1·7013	1·3
				1·7020§	2·0
Liver	24·5	11·4	1·7007	1·7008	0·1
				1·7020§	1·3
Thymus	21	7·8	1·7008	1·7013	0·5
				1·7020§	1·2
Liver	12·5	1·8	1·7008	1·7008	0

† Molecular weights calculated from the $s_{20,w}$ values using the relationship of Eigner & Doty (1965): thus M_w is the weight average molecular weight.

‡ The error on the ρ_0 values is $\pm 0{\cdot}0005$ g/cm^3; that on the $\langle\rho\rangle$ values is $\pm 0{\cdot}0002$ g/cm^3.

§ $\langle\rho\rangle$ and $\langle\rho\rangle - \rho_0$ values calculated for main band DNA, not taking into account the contribution of the light satellite.

leads to the appearance of material banding at as high as 1·715 g/cm^3. This is an effect not simply due to band widening because of the decrease in molecular weight, but also to the upward shift in buoyant density of the 1·709 g/cm^3 component after degradation (Fig. 6).

Concerning the satellite DNA, it should be noted that its separation from the main band shows an improvement as the DNA molecular weight increases from $1{\cdot}8 \times 10^6$

TABLE 5

Component patterns of mouse thymus DNA (CsCl analysis)

$s_{20,w}$	M_w ($\times 10^{-6}$)	Major components (ρ)	(%)		Minor components and satellites (ρ)	(%)
50	66·2	1·699	44	68	1·691	6
		1·7015	24			
		1·7045	22			
		1·7090	3			
21†	7·8	1·699	35	61	1·691	7
		1·7015	26		1·695	2
		1·7045	24		1·713	2
		1·709	5			

† This DNA preparation was obtained by syringe shearing of the 50 S preparation.

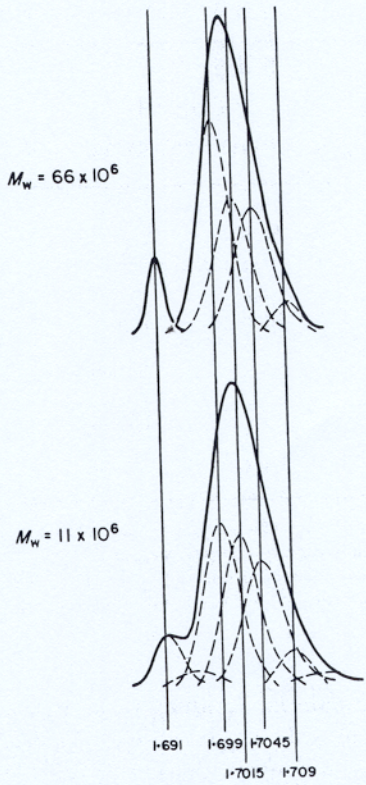

FIG. 7. CsCl analysis of 2 DNA samples from mouse thymus at different molecular weights. Molecular weights are measured from sedimentation velocity experiments. The lower molecular weight sample was obtained by syringe shearing of the high molecular weight sample.

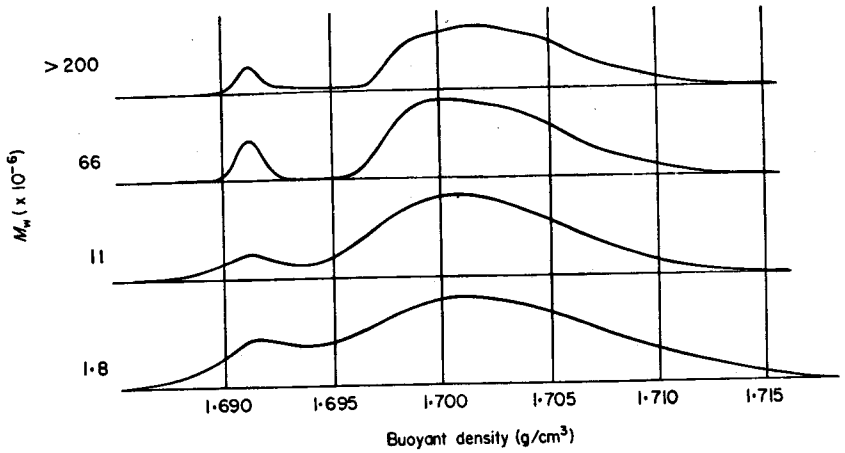

FIG. 8. Analytical CsCl density gradient profiles of 4 mouse DNA samples of different molecular weight.
Molecular weights are measured from sedimentation velocity experiments except for the highest one (see Results, section (d)).

to 66×10^6, in the latter case the separation being complete, this effect is expected because of the band narrowing due to the increased molecular weight. It is worth noting, however, that in the highest molecular weight preparation, material trailing from the satellite peak into the main band can be seen, indicating that at this very high molecular weight, interspersion of satellites and main band material begins to be seen.

4. Conclusions

The present work has led to three major conclusions on the organization of the eukaryotic genomes at a macromolecular level. The first one is that some main band DNAs, like those of *S. cerevisiae* and *D. melanogaster*, do not exhibit components which can be separated from each other on the basis of the preferential binding of silver ions. In the preceding paper it was shown that these genomes had symmetrical main bands, when examined at a molecular weight level of 16×10^6. Here, evidence has been obtained for the lack of distinguishable components at a molecular weight as low as 1×10^6. In this respect DNAs from *S. cerevisiae* and *D. melanogaster*, two species characterized by very small *c*-values, do not differ from *E. coli* DNA. In contrast with *Drosophila* DNA, degraded crab DNA exhibits two major components in addition to the main component. Unavailability of high molecular weight crab DNA has prevented us from establishing whether these components are interspersed with each other at a molecular weight of 10^7 or more.

The second conclusion is that the discrete components forming the main band of mammalian DNAs (Filipski *et al.*, 1973 and Thiery *et al.*, 1976) exhibit very little or no intermolecular heterogeneity once they are degraded by *Hin*dII + III to molecular sizes in the 1×10^6 to 2×10^6 range. In contrast with this result, amphibian DNAs showed a rather drastic change in their component patterns at a low compared to a high molecular weight level. Changes in buoyant densities and amounts of some components, the disappearance of other components and the appearance of new ones were observed.

The third conclusion, which is limited to the mouse genome, but is probably valid for all mammalian genomes, is that increasing the molecular weight of DNA over and above 200×10^6, though causing the appearance of a beginning of interspersion of satellite with main band DNA, does not seem to have much effect on the major components, as indicated by the appearance of maxima on the CsCl profile which correspond to the buoyant density of the various components, and by the apparent absence of a decrease in the compositional heterogeneity of the DNA. Although some degree of interspersion cannot be ruled out, these observations point to the existence of the major components in very large, continuous blocks. A detailed study of isolated components is under way in our laboratory.

APPENDIX

(a) *Analysis of DNA buoyant density profiles in CsCl*

As clearly shown by the results of the preceding paper, mammalian DNAs typically show asymmetric buoyant density profiles when centrifuged to equilibrium in CsCl density gradients. If such asymmetric distributions arise from the superposition of a number of symmetric distributions then the resolution of the profile in a number of symmetrical curves is unique (Medgyessy, 1961). We have indeed indications from our previous work (Filipski *et al.*, 1973 and Thiery *et al.*, 1976, Figs 1 to 3) that fractionation of mammalian DNAs in Cs_2SO_4–Ag^+ density gradients leads to the preparation of DNA components which show symmetrical profiles when centrifuged in CsCl density gradients (see for instance, fractions 2 and 3 in Fig. A1(a)).

In our Gaussian analysis of buoyant density profiles the basic criterion for a unique resolution is, therefore, considered satisfied. We have, however, imposed two additional restrictions: the first is that the standard deviations of the Gaussian components are in agreement with the molecular weight of the fraction under consideration, the latter being determined from the sedimentation coefficient of the fraction; the second is that Gaussian DNA component, as characterized by its buoyant density, is present in several neighboring Cs_2SO_4–Ag^+ fractions and its amount in these fractions go through a maximum. It should be noted that these restrictions overdetermine the Gaussian analysis of eukaryotic genomes by the combined Cs_2SO_4–Ag^+, CsCl approach.

We will give here an example of the procedure used. Examination of the profiles in Figure A1(a) shows that two fractions, 2 and 3, have profiles with the same modal buoyant density, 1·699 g/cm^3. The measurement of the sedimentation coefficient for both fractions gives almost identical $s_{20,w}$ values (25 S $\pm$ 1 S). One single Gaussian curve can be fitted under these two profiles, with the same standard deviation and the same mode, 1·699 g/cm^3; the area under the curve represents more than 90% of the total surface. Thus, the existence of a component of density 1·699 g/cm^3 is evident.

A single Gaussian curve can be fitted under the profile of fraction 4, with a maximum at 1·7005 g/cm^3; its standard deviation is, however, too large, on the basis of the molecular weight calculated for that fraction from the $s_{20,w}$ value (25 S). Also, by the criteria described above, the 1·699 g/cm^3 component, present in fractions 2 and 3 should be present in fraction 4 (and in fraction 1 as well); a Gaussian curve having

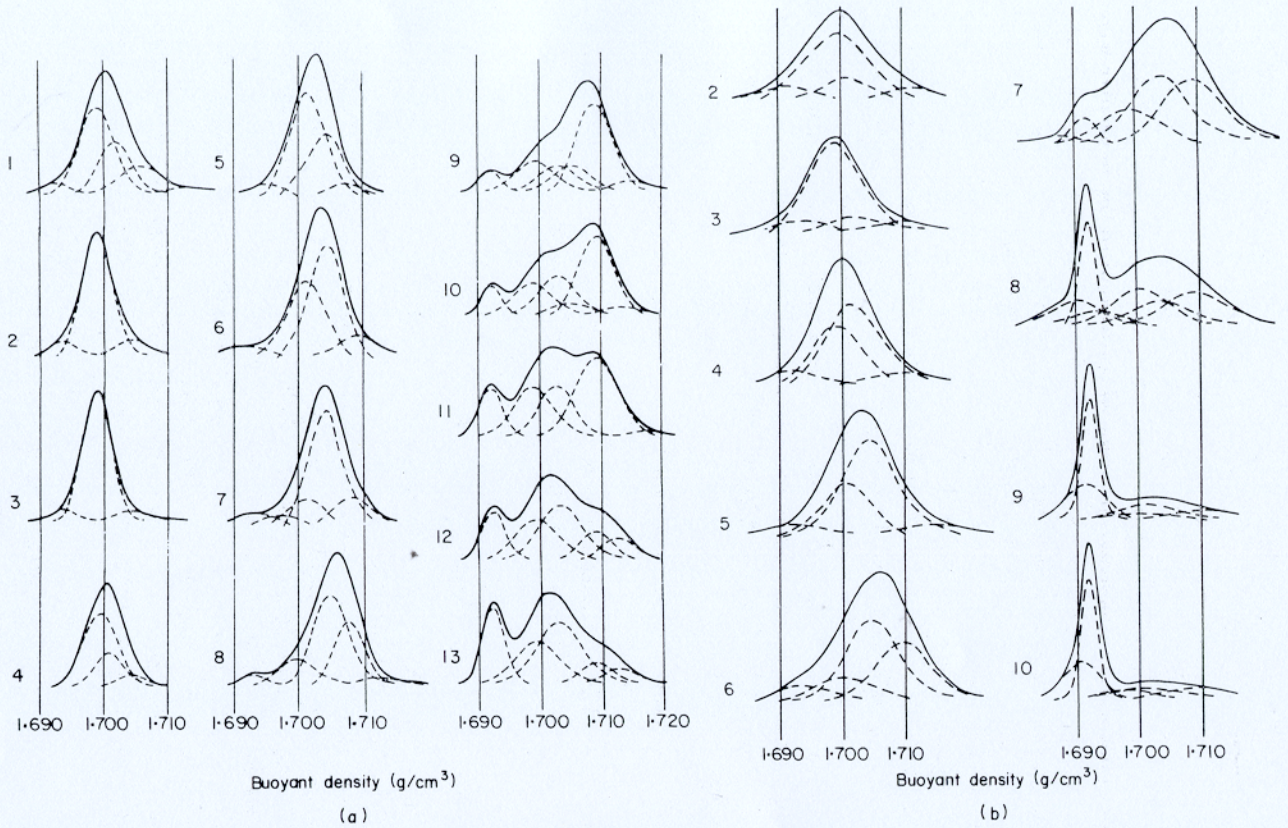

FIG. A1. Analytical cesium chloride density gradient profiles of fractions from (a) undegraded (Fig. 2 of the Thiery *et al.*, 1976), and (b) degraded (Fig. 1, this paper) mouse liver DNA. Gaussian curves (broken lines) represent the different DNA components as resolved using a Dupont 310 curve resolver and the criteria given in Appendix, section (a).

a standard deviation corresponding to the molecular weight of the fraction and a mode at 1·699 g/cm³ can be fitted under the profiles; the area defined by this curve represents 70% of the total surface of the band; the only way to fill in this surface is by fitting in it two more Gaussian curves with modes at about 1·701 and 1·705 g/cm³.

A similar analysis applied to fractions 5 and 6 confirms the existence of these two components, 1·701 and 1·705 g/cm³. In fraction 7, the profile can be fitted with a single Gaussian curve, with a mode at 1·705 g/cm³; the small shoulder on the left is fitted by a curve at 1·692 g/cm³. The Gaussian curve thus fitted at 1·705 g/cm³ has a standard deviation too large compared to the molecular weight of the fraction (24 S). If its standard deviation is decreased in order to correspond to the molecular weight of the fraction, two new components should be added to fill in the surface, one at 1·7015 g/cm³ and the other at 1·709 g/cm³. The presence of a 1·7015 g/cm³ component in fraction 7 is not surprising in view of its existence in fractions 4, 5 and 6. A recurrent analysis of the kind just described for some of the fractions leads to a unique solution for all the components of Figure A1(a).

Figure A1(b) shows a similar analysis for the mouse DNA after degradation by restriction enzymes *Hin*dII + III. This is presented for the sake of comparison of the components as present in undegraded and degraded DNA. An additional reason of interest is the evidently sharper peak corresponding to the "satellite" in the degraded as compared to the undegraded sample (compare Fig. A1(a), fractions 10 to 13, with Fig. A1(b), fractions 8 to 10). An explanation for this phenomenon is given in section (c), below.

(b) *Molecular weight and total heterogeneity calculations from density gradient sedimentation equilibrium*

In the case of a DNA homogeneous in buoyant density, an apparent molecular weight, $M_{3\text{app}}$, can be calculated from its distribution in a density gradient

$$\frac{1}{M_{3\text{app}}} = G\left(\frac{\omega^4 r_0^2}{RT\rho}\right)\langle\delta^2\rangle_{\text{app}}, \tag{1}$$

where R is the gas constant, T the absolute temperature and G, a parameter associated with the effective density gradient, is given by $G = 1 + \Gamma'/\beta_{\text{eff}}$ (Schmid & Hearst, 1971). The true molecular weight, M_3, is determined experimentally by extrapolation of the apparent molecular weight to zero concentration. In our hands, T7 DNA gives a molecular weight of $24{\cdot}8 \times 10^6$ in excellent agreement with that given by Schmid & Hearst (1969) using the same technique.

In the case of a DNA heterogeneous in buoyant density the variance of the distribution may be assumed to be the sum of a contribution from diffusion and a contribution from density heterogeneity, if there is no correlation between density heterogeneity and molecular weight heterogeneity (Sueoka, 1959):

$$\frac{1}{M_{\text{app}}} = \frac{G\omega^4 r_0^2 \langle\delta^2\rangle}{RT\rho} = \frac{1}{M_3} + \left(\frac{G\beta_{\text{B}}^2 a^2}{RT\rho}\right)\langle(\text{GC})^2\rangle, \tag{2}$$

β_{B} is related to the buoyancy gradient, a is the slope of the plot of buoyant density against GC content for a given salt solution, $\langle(\text{GC})^2\rangle$ is the variance of the GC composition (Schmid & Hearst, 1972).

Equation (2) may be used to estimate the effect of the GC variance on the ratio

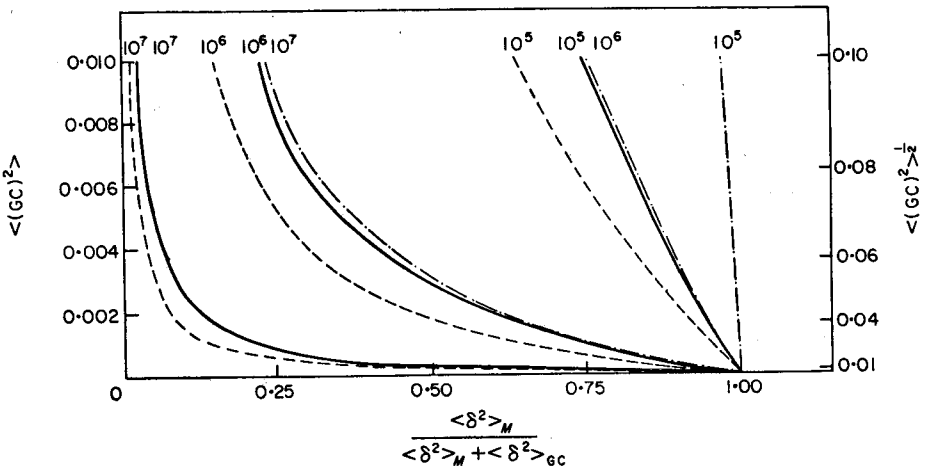

FIG. A2. Plot of the variance of base composition (expressed as G + C molar fraction) *versus* the ratio of the variance of the diffusion spreading $\langle\delta^2\rangle_M$ over the total variance of the profile $\langle\delta^2\rangle_T$. Theoretical curves have been calculated after eqn (2) (Schmid & Hearst, 1972) at 3 different molecular weights (10^5, 10^6 and 10^7) and for 3 buoyant media: Cs_2SO_4 (—·—·—), CsCl (————) and CsHCOO (– – – – –).

of the variance due to diffusion $\langle\delta^2\rangle_M$ over the total variance of the band $\langle\delta^2\rangle_T$. As shown in Figure A2 a small GC variance causes a stronger change in the total variance if the molecular weight is higher; such an effect is much stronger in Cs formate and CsCl than in Cs_2SO_4 (Schmid & Hearst, 1971).

The molecular weights determined by equations (1) and (2) are number-average molecular weights. If σ^2 (σ being the standard deviation, as measured at 0·606 of peak height) is used instead of $\langle\delta^2\rangle$, weight-average molecular weights are obtained.

Equation (2) can be used to estimate the total buoyant density heterogeneity of a DNA sample, if its number average molecular weight is known. If not, the apparent molecular weight can be measured (extrapolated to infinite dilution) in two or more Cs salt systems and plotted according to equation (2); the slope of a $1/M_{3\text{app}}$ *versus* $G\beta_B^2a^2/RT\rho$, giving the heterogeneity, and the intercept $1/M_3$, the true molecular weight.

(c) *Aggregation phenomena in satellites DNAs*

Satellite DNAs usually show up in CsCl density gradients as sharp bands. This behaviour has been usually attributed to their high compositional homogeneity. The data presented below show that this explanation is not fully satisfactory.

Purified mouse satellite DNA was centrifuged to equilibrium in CsCl at different DNA concentrations and its weight average molecular weight was calculated using equation (1) and extrapolation to infinite dilution. The extrapolated molecular weight was found to be $38{\cdot}9\times10^6\pm1{\cdot}1\times10^6$. The weight average molecular weight was measured independently by boundary sedimentation velocity. The $s^{50\%}_{20,w}$ value calculated was 25·2 S ± 0·46 S, extrapolated to infinite dilution. Using the *s versus M* relationship of Eigner & Doty (1965), an M_w value of $12{\cdot}2\times10^6$ was obtained. This value is much lower than $38{\cdot}9\times10^6$, measured by sedimentation equilibrium in CsCl. Now, this latter value, if anything, may be slightly underestimated because of a possible compositional heterogeneity in mouse satellite DNA.

It is conceivable that the aggregation phenomenon described here is due to concatenation by intermolecular base-pairing in single-stranded ends protruding from the satellite DNA fragments, since Pyeritz *et al.* (1971) observed that under annealing conditions, sheared mouse satellite DNA shows over 20% circular molecule formation. The single-stranded ends created by the shearing procedure were responsible for this cyclization. A similar phenomenon has been observed by Schmid & Hearst (1972) in λ DNA, where the cohesive ends were responsible for the aggregation. A very strong evidence in support of a single-stranded end aggregation comes from the results of Figure A1(a) and (b). The satellite DNA degraded by *Hind*II + III which exhibits an $s_{20,w} = 18$ (this was determined for fraction 10 of Fig. A1(b)) shows a much sharper peak than that present in the undegraded DNA ($s_{20,w} = 21$; fraction 13 of Fig. A1(a)). The production of sticky ends by *Hind*III and the consequent concatenation appear to be the only explanation for this phenomenon.

We thank Dr H. Kopecka of our laboratory for the generous gift of *Hind*II+III.

REFERENCES

Bernardi, G., Piperno, G. & Fonty, G. (1972). *J. Mol. Biol.* **65**, 173–189.
Eigner, J. & Doty, P. (1965). *J. Mol. Biol.* **12**, 549–580.
Filipski, J., Thiery, J. P. & Bernardi, G. (1973). *J. Mol. Biol.* **80**, 177–197.
Kopecka, H. (1975). *Biochim. Biophys. Acta*, **391**, 109–120.
Medgyessy, P. (1961). *Decomposition of Superpositions of Distribution Functions*, Publishing House of the Hungarian Academy of Sciences, Budapest.
Peacock, W. J., Brutlag, D., Goldring, E., Appels, R., Hinton, C. W. & Lindsley, D. L. (1973). *Cold Spring Harbor Symp. Quant. Biol.* **38**, 405–416.
Pyeritz, R. E., Lee, C. S. & Thomas, C. A., Jr (1971). *Chromosoma*, **33**, 284–296.
Schmid, C. W. & Hearst, J. E. (1969). *J. Mol. Biol.* **44**, 143–160.
Schmid, C. W. & Hearst, J. E. (1971). *Biopolymers*, **10**, 1901–1924.
Schmid, C. W. & Hearst, J. E. (1972). *Biopolymers*, **11**, 1913–1918.
Skinner, D. M. (1967). *Proc. Nat. Acad. Sci., U.S.A.* **58**, 103–110.
Skinner, D. M. & Kerr, M. J. (1971). *Biochemistry*, **10**, 1864–1872.
Smith, H. & Nathans, D. (1973). *J. Mol. Biol.* **81**, 419–423.
Smith, H. O. & Wilcox, K. W. (1970). *J. Mol. Biol.* **51**, 379–391.
Sueoka, N. (1959). *Proc. Nat. Acad. Sci., U.S.A.* **45**, 1480–1490.
Thiery, J. P., Macaya, G. & Bernardi, G. (1976). *J. Mol. Biol.* **108**, 219–235.
Zubay, C. & Doty, P. (1959). *J. Mol. Biol.* **1**, 1–20.